How Anion Chaotrope Changes the Local Structure of Water: Insights from Photoelectron Spectroscopy and Theoretical Modeling of SCN−·Water Clusters

ARTICLE *in* THE JOURNAL OF PHYSICAL CHEMISTRY B · SEPTEMBER 2015

Impact Factor: 3.3 · DOI: 10.1021/acs.jpcb.5b07257

THE JOURNAL OF PHYSICAL CHEMISTRY B

Article

pubs.acs.org/JPCB

How Anion Chaotrope Changes the Local Structure of Water: Insights from Photoelectron Spectroscopy and Theoretical Modeling of SCN^- Water Clusters

Marat Valiev,*[,†] Shihu H. M. Deng,[‡] and Xue-Bin Wang*[,‡]

[†]Environmental Molecular Sciences Laboratory, Pacific Northwest National Laboratory, P.O. Box 999, Richland, Washington 99352, United States

[‡]Physical Sciences Division, Pacific Northwest National Laboratory, 902 Battelle Boulevard, P.O. Box 999, MS K8-88, Richland, Washington 99352, United States

Supporting Information

ABSTRACT: The behavior of charged solute molecules in aqueous solutions is often classified using the concept of kosmotropes ("structure makers") and chaotropes ("structure breakers"). There is a growing consensus that the key to kosmotropic/chaotropic behaviors lies in the local solvent region, but the exact microscopic basis for such differentiation is not well-understood. This issue is examined in this work by analyzing size selective solvation of a well-known chaotrope, a negatively charged SCN^- molecule. Combining experimental photoelectron spectroscopy measurements with theoretical modeling, we examine evolution of solvation structure up to eight waters. We observe that SCN^- indeed fits the description of weakly hydrated ion, and its solvation is heavily driven by stabilization of water−water interaction network. However, the impact on water structure is more subtle than that associated with "structure breaker". In particular, we observe that the solvation structure of SCN^- preserves the "packing" structure of the water network but changes local directionality of hydrogen bonds in the local solvent region. The resulting effect is closer to that of "structure weakener", where solute can be readily accommodated into the native water network, at the cost of compromising its stability due to constraints on hydrogen bonding directionality.

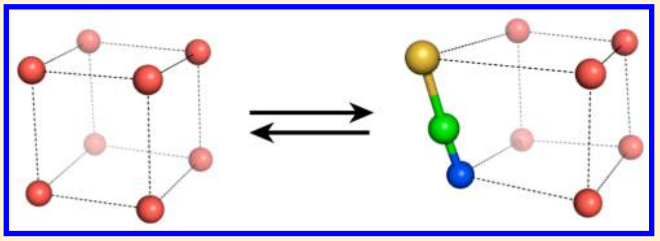

INTRODUCTION

Fundamental understanding of aqueous solutions containing complex charged species is a problem of great scientific and practical interest.[1−5] One of the most interesting and highly debated topics in this area involves the so-called solute specific effect[3,6,7] − phenomena where different solute molecules within the same charge family exhibit markedly different solvation characteristics. A well-known example of such behavior can be found in the much discussed Hofmeister series.[1,2] While these effects have been documented both experimentally[2] and through simulations,[6,7] a precise source of differences is not fully understood. One of the important findings was that a continuum model approach, where solvent is represented by a homogeneous dielectric medium, is likely to be inadequate, and molecular level details are required.[8] In particular, it is now believed that solute specific effects arise from the particular changes in aqueous hydrogen bonding network brought in by the insertion of the solute.[9,10] This notion is captured in the now commonly used classification of solutes into "kosmotropes"/"structure makers" and "chaotropes"/"structure breakers".[2,11] These concepts are meant to bridge macroscopically observed Hofmeister series with molecular level description, but there is some ambiguity regarding the actual meaning of structure making and breaking.[11] Other definitions based on strength of ion−water interactions can be adopted,[8] but the question of how different types of charged solutes affect the structure of water remains open and bears important implications for fundamental understanding of solute specific effects.

Spectroscopic measurements of bulk solution[12] have indicated that neither kosmotropic nor chaotropic species have a significant effect on the bulk solvent region outside the immediate vicinity of the solute. This suggests that the origin of solute specific effects lies in the molecular properties of the local solvent region,[2,12−14] where the two opposing parts of the systems, solute and bulk environment, come to interact with each other. The solute tries to organize the nearby water molecules according to its internal geometry and charge distribution, whereas the bulk environment resists this change attempting to maintain bulk-like structure. The end balance is likely to be a sensitive function of solute geometry and charge distribution.[10] In this view, kosmotropic solute might be considered highly incompatible with native bulk water

Special Issue: Bruce C. Garrett Festschrift

Received: July 27, 2015
Revised: September 2, 2015

DOI: 10.1021/acs.jpcb.5b07257
J. Phys. Chem. B XXXX, XXX, XXX−XXX

structure, and significant structural rearrangements of the local solvent region would be required to encapsulate its effect on the rest of the system. This is consistent with the previously proposed description of kosmotropes as forming effective rigid solute−water particles suspended in bulk water.[12] For chaotropes the situation is less clear. They are described as weakly hydrated implying that solvent−solvent interactions are of greater importance,[8] but what precipitates such behavior from the molecular point of view is less clear. To further understand this issue requires precise characterization of the solute−solvent interaction and how they and resulting properties of local solvent structure are affected by particular solute characteristics. One promising approach to this problem can be found in the studies of solvated clusters.[15−30] The absence of the bulk solvent environment amplifies effects of solute−solvent interactions exposing a level of detail that may not be possible to resolve in bulk observations.

Our approach to cluster solvation studies integrates both experimental and theoretical modeling components. On the experimental side, we use photoelectron spectroscopy (PES)[15−17] techniques to measure spectroscopic signature of size selective aqueous clusters. This information is then integrated with ab initio calculations to gain deeper fundamental understanding of the experimental data. One of the quantities that can be obtained from PES spectra is vertical detachment energy (VDE), which is defined as an energy difference between charged and neutral states of the cluster (with n solvent water molecules),

$$\mathrm{VDE}(n) = E^{\mathrm{neutral}}(n) - E^{\mathrm{anion}}(n)$$

The important characteristic of VDE is that it is a sensitive function of the solvent environment. Serving as spectroscopic signature, it is often used to uniquely identify the structure of the observed cluster.[15−17,31,32] The importance of VDE is not limited to structural predictions, and its behavior as a function of cluster size holds important clues regarding the energetics of the solvation process. A case in point can be found in the solvation of iodate anion (IO_3^-), where an anomaly in the VDE evolution was connected to the strong solvent organizing properties of the solute.[15] This is consistent with classification of iodate as a strong kosmotrope.[9] The interesting question is then how different the cluster solvation would be for a chaotrope anion. After all, if distinctive behavior of kosmotropes and chaotropes stems from the specific properties of the local properties,[10] such differences should be amplified in the cluster solvation process. This is the issue addressed in the present work where we study cluster solvation behavior of thiocyanate (SCN^-), a linear rigid anion solute, whose behavior in aqueous solution is considered to be that of a chaotrope.[2,10]

PHOTOELECTRON SPECTROSCOPY

The PES experiments were performed with a low-temperature, magnetic-bottle time-of-flight photoelectron spectrometer, coupled to an electrospray ion source (ESI) and a temperature-controllable cryogenic ion-trap.[33] $SCN^-(H_2O)_n$ clusters were produced by electrospraying into the gas phase a 0.1 mM solution of NaSCN (or KSCN), dissolved in mixed H_2O/CH_3CN (1/3) solvent. The anions generated were guided by quadrupole ion guides into a cryogenic ion trap, where the anions were trapped for 20−100 ms and cooled by collisions with buffer gas molecules. In the current study, the trap temperature was set to 20 K. The cooling of the clusters to 20 K eliminated the possibility of the appearance of extra spectral peaks in the PES spectra, due to hot bands, and minimized the possible isomers that might exist in the ion beam. These anion clusters were then mass-selected and decelerated before being photodetached with a laser beam at 157 nm (7.867 eV) from an F_2 excimer laser. The laser was operated at a 20 Hz repetition rate with the ion beam off at alternating laser shots to enable shot-to-shot background subtraction to be carried out. Photoelectrons were collected at ∼100% efficiency with the magnetic bottle and analyzed in a 5.2 m long electron flight tube. The time-of-flight photoelectron spectra were collected and converted to kinetic energy spectra, calibrated by the known spectra of I^- and $Cu(CN)_2^-$. The electron binding energy spectra were obtained by subtracting the kinetic energy spectra from the detachment photon energy. Although the spectrometer has a resolution (ΔE/kinetic energy) of ∼2% or 20 meV for electrons with 1 eV of kinetic energy for the intense anions, all spectra of $SCN^-(H_2O)_n$ (n = 0−8) were taken here under a compromised but identical condition, i.e., with a resolution of ∼3% for 1 eV kinetic energy of electrons in order to unravel underlying spectral width as a function of water. The experimental value of VDE was obtained from the maximum of the first peak in each spectrum.

THEORETICAL METHODS

All the calculations were performed using the NWChem computational chemistry package.[34] Structural optimizations were based on the DFT/B3LYP level of theory[35,36] and 6-31++G** basis set.[37,38] An initial set of cluster structures was generated manually. These were then expanded using a genetic optimization algorithm, whereby an offspring structure is formed from two parent structures based on geometrical arguments as described by Alexandrova.[39] This initial offspring structure is then used to generate an ensemble of structures that differ by the directions of the hydrogen bonds. A more detailed description of the procedure will be presented elsewhere. Charge analyses of resulting configurations were performed with the NBO[40] module within NWChem. The theoretical VDE was calculated as the energy difference between the doublet neutral and singlet anion species, both at the same optimized anion geometry.

EXPERIMENTAL RESULTS

The T = 20 K PES spectra of $SCN^-(H_2O)_n$ (n = 0−8) at 157 nm are shown in Figure 1. All spectra are similar, each exhibiting one strong peak with a second, well-separated weak band at high binding energy. The measured VDE of SCN^-, 3.55 eV, is consistent with previous studies.[41,42] The spectra of $SCN^-(H_2O)_n$ show a steadily stepwise blue shift in binding energy for n = 0 to 5 as expected. The spectrum of $SCN^-(H_2O)_6$, however, exhibits a surprise in that it has almost an identical VDE to that of n = 5, followed by continuous blue shift in energy for n = 7 and 8 (Table 1 and Figure 2). Close examination of all spectra unravels an interesting variation on the spectral bandwidth (full width at half-maximum, fwhm) with addition of each water molecule: the fwhm(n) of $SCN^-(H_2O)_n$ shows a gradual increase from n = 0 to 5, but a sudden decrease at n = 6, followed by appreciable increases for n = 7 and 8 (Figure 2). In general, the spectral bands of clusters are expected to get broader with addition of each water molecule, due to the extra solvent coordinates introduced in the cluster anions and possible coexistence of multiple isomers. It is

DOI: 10.1021/acs.jpcb.5b07257
J. Phys. Chem. B XXXX, XXX, XXX−XXX

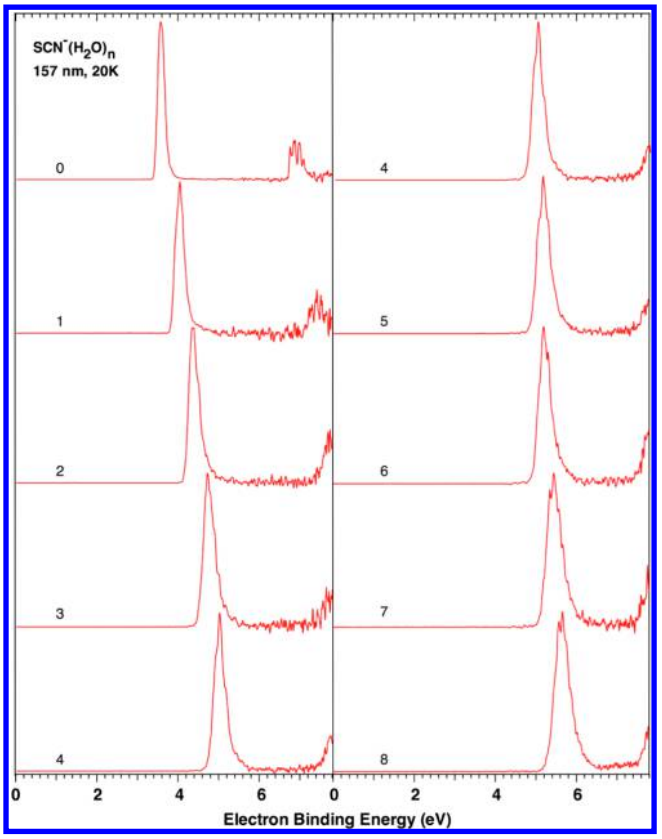

Figure 1. 20 K PES spectra of $SCN^-(H_2O)_n$, n = 0−8 at 157 nm (7.867 eV).

Table 1. Experimental and Calculated Vertical Detachment Energies (VDEs) and Full Width at Half Maximum (fwhm) of the Main Spectral Peak of $SCN^-(H_2O)_n$ (in eV)

n	expt[a]	calcd[b]	fwhm[e]
0	3.55(1)	3.52	0.21(1)
1	4.03(2)	4.02	0.25(1)
2	4.35(2)	4.40	0.29(1)
3	4.71(2)	4.73	0.31(1)
4	5.01(2)	5.03	0.31(1)
5	5.18(2)	5.18	0.34(1)
6	5.19(2)	5.19	0.32(1)
7	5.43(4)	5.26, 5.46[c]	0.43(1)
8	5.66(4)	5.32, 5.53[d]	0.43(1)

[a]Obtained from the maximum of the first peak from each spectrum. Numbers in parentheses represent experimental uncertainty in last digits. [b]Calculated as energy difference of the doublet neutral and singlet anion states both at the optimized anion geometry with the lowest energy at the DFT/B3LYP/6-31++G** level of theory (see Figures 3−5 for the lowest energy structures for each cluster). [c]From an isomer lying 1.2 kcal/mol higher in energy than the lowest one (Figure 5) . [d]From an isomer lying 0.04 kcal/mol higher in energy than the lowest one (Figure 5). [e]Full width at half-maximum for the first peak from each spectrum. Numbers in parentheses represent experimental uncertainty in last digits.

certainly unexpected to see a drop of spectral bandwidth at n = 6 from n = 5. It is also worth noting that the spectral band for n = 7 and 8 is significantly broader than that at n = 6. Thus, our PES study seems to suggest $SCN^-(H_2O)_6$ with a special trait en route solvation evolution, which is born out from our theoretical calculations that show $SCN^-(H_2O)_6$ forms an almost perfect cubic structure with a special stability (vide infra).

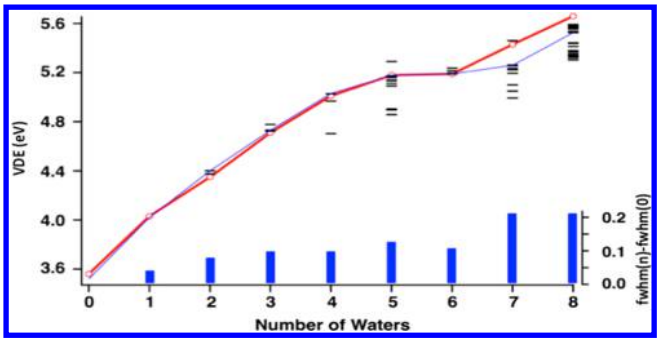

Figure 2. Vertical detachment energies (VDEs) of SCN^- water cluster. Experimental data is shown by the red line with circle markers. VDE values for lowest energy calculated clusters are shown by a thin blue line. Calculated VDE values for all the clusters within 1.2 kcal/mol of the lowest energy clusters (see the Supporting Information) are also shown using horizontal bars. The full widths at half-maximum (fwhm) of $SCN^-(H_2O)_n$ relative to that of SCN^- are displayed as vertical blue bars.

THEORETICAL RESULTS AND DISCUSSIONS

Analysis of Low-Energy Isomers. The optimized structure of SCN^- molecule in the gas phase is shown in Figure 3. It is a linear molecule with calculated C−N and C−S

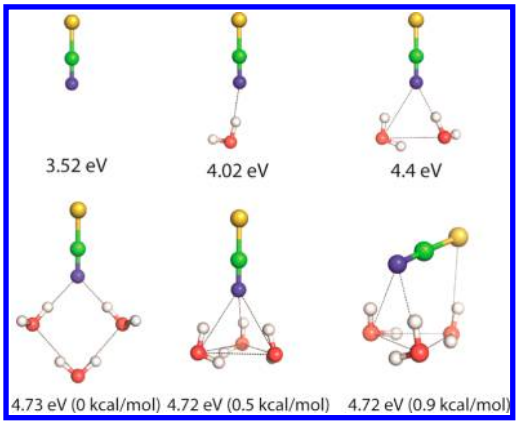

Figure 3. Optimized structures of the lowest energy isomers of the n = 0−3 clusters. N in blue, C in green, S in yellow, O in red, and H in gray are used for all images. Calculated VDEs (eV) and relative energy (kcal/mol in parentheses) for each structure are indicated.

bond lengths of 1.18 and 1.67 Å correspondingly. According to charge population analysis the excess negative charge is nearly equally distributed between N (−0.58) and S atoms (−0.46). This implies that in the course of solvation both ends of the molecule can serve as potential interaction points with solvent water molecules. After the electron ejection, both of the atoms lose some portion of electron density. However, the sulfur atom is impacted the most, which leads to significant changes in the charge distribution; the nitrogen site remains negatively charged (−0.23), but the sulfur end becomes positively charged (0.27).

The lowest energy three-dimensional structures of solvated SCN^-−water clusters, as identified in our calculations, are shown in Figures 3−5. While for small SCN^-−water clusters, explicit three-dimensional representation is relatively easy to

DOI: 10.1021/acs.jpcb.5b07257
J. Phys. Chem. B XXXX, XXX, XXX−XXX

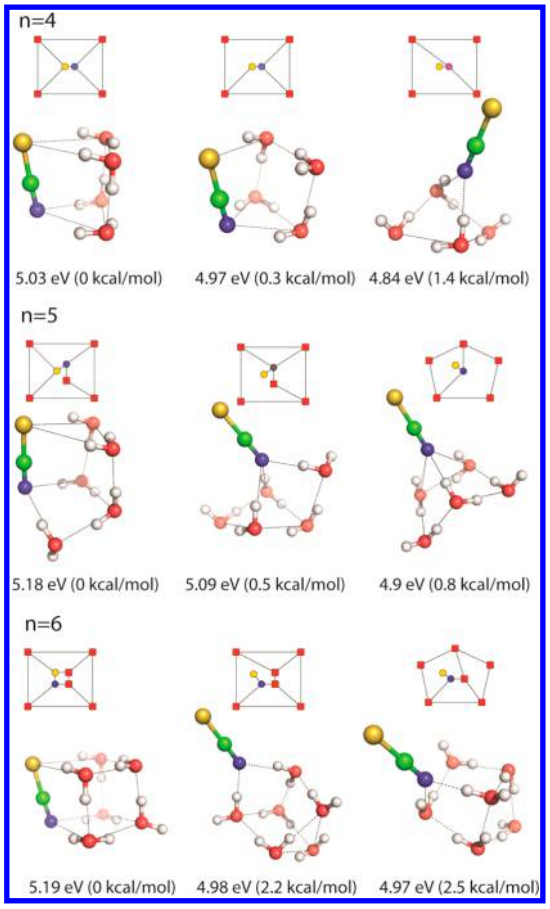

Figure 4. Optimized structures of the lowest energy isomers for the n = 4−6 clusters. N in blue, C in green, S in yellow, O in red, and H in gray are used for all images. Calculated VDEs (eV) for each structure and relative energy (kcal/mol) are indicated. Graph presentation of connectivity is provided on top of each 3-D structure.

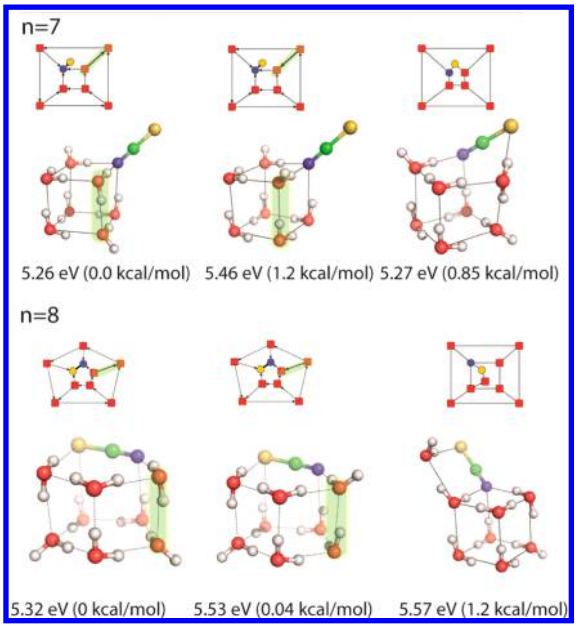

Figure 5. Optimized structures of the lowest energy isomers for the n = 7−8 clusters. N in blue, C in green, S in yellow, O in red, and H in gray are used for all images. Calculated VDEs (eV) for each structure and relative energy (kcal/mol) are indicated. Graph presentation of connectivity is provided on top of each 3-D structure. The differences in hydrogen bonding between similar structures are highlighted.

understand, the complexity increases significantly with the system size. A simpler way to describe and characterize structures would be advantageous at this point. One common strategy, which is often utilized, is based on describing structures in terms of mutual proximities of the constituent particles or packing (e.g., "book" structure in water clusters).[43,44] For hydrogen bonding species, an additional description involving mutual orientation is also utilized (e.g., hydrogen donors/acceptors patterns).[45,46] These concepts proved to be quite useful in conveying underlying features of cluster formation, but the inherent naming ambiguity does not easily lend itself to the discussion of larger structures or automated processing. It is for these reasons that in the course of this work we found it useful to utilize graph-based representation of three-dimensional cluster structures. Such representation is aimed to capture only the essential connectivity aspects of the underlying three-dimensional structure and offers a surprisingly complete way to classify underlying cluster structures. Each node on the graph denotes water or solute molecule (SCN^-), and the connection or edge between the two nodes is formed if the two molecules are located within a certain cutoff distance of each other. In our case, the waters were considered connected if O−O distance was less than 3.0 Å. The connection between SCN^- and water was based on N−O distance of 3.3 Å and S−O distance of 3.8 Å. These rules give rise to the so-called undirected graph representations of cluster structures and provide one particular way to quantify overall arrangement/packing motifs. In particular, for a given cluster size all the stable cluster configurations can be classified into unique packing classes based on graph isomorphism. The graphs are considered isomorphic ("equal") if they can be transformed into each other without change in the connectivity. Each graph can give rise to many possible *stable* cluster structures, which, in our experience, present different realizations of possible hydrogen bonding network and not different spatial arrangements. The actual concept of hydrogen bonding network can also be captured by the extension to *directed* graphs, whereby each edge is assigned a direction based on hydrogen bond donor/acceptor assignments. Once the uncertainty regarding the hydrogen bond network is removed, each directed graph representation has so far resulted in a *unique* three-dimensional realization of stable cluster structure.

$SCN^-(H_2O)_{0-3}$. The lowest energy three-dimensional structures of solvated SCN^-−water clusters with up to three waters are shown in Figure 3. We observe that, in the initial stages of solvation of SCN^- (n = 1−2), the evolution of cluster structures is driven by the coordination of nitrogen site. The latter has a smaller size compared to that of a comparably charged sulfur atom, which allows for closer approach by water molecules (R_{NO} ∼ 2.8 Å versus R_{SO} ∼ 3.6 Å) enhancing solvation effects. For example, in the n = 2 case, we do find the structure where both the nitrogen and sulfur ends of the molecule are coordinated; it is however ∼1 kcal/mol higher in energy compared to the nitrogen only coordinated case. Beyond two waters the advantage for nitrogen coordination becomes less clear. Indeed for n = 3 cluster the additional water has several competing choices. In the lowest energy structure it enters the second solvation shell leaving solute coordination unchanged. The next lowest energy structure (+ 0.5 kcal/mol) involves adding to coordination of the nitrogen site (3-fold).

DOI: 10.1021/acs.jpcb.5b07257
J. Phys. Chem. B XXXX, XXX, XXX−XXX

The final option (+0.9 kcal/mol) involves solvation of both N (2-fold) and S (1-fold). In all three cases the VDE values are similar to each other (~4.7 eV) and match the experimental data.

$SCN^-(H_2O)_4$. Starting with the n = 4 cluster, the water molecules have the opportunity to coordinate the sulfur site. From the geometrical point of view the lowest energy structure takes the shape of a trigonal prism, with one of the sides represented by SCN^-. The sulfur site can in this case assume 2-fold (lowest energy) or 1-fold coordination (~0.3 kcal/mol), with both structures providing nearly the same VDE value for this structure and in good agreement with the experimental data. From the connectivity point of view, as provided by graph representations, we observe that the main motif in the lowest energy structures is the embedding of SCN^- into the cyclic 4-ring water network. The lowest energy structure corresponds to the fully embedded case, where both nitrogen and sulfur ends are 2-fold coordinated to the water ring network. Given the highly connected nature of this structure, it has only one possible realization of the hydrogen bonding network. From that structure progressively high-energy structures can be generated by gradual removal of SCN^-–water edges. This reduction in coordination involves the sulfur site, whose interaction with solvent, as noted earlier, is the weakest.

$SCN^-(H_2O)_5$. In the n = 5 case the trigonal prism is starting to be transformed into its cubic analogue. The lowest energy cluster is essentially generated from n = 4 cluster by the insertion of water into the base of the pyramid on the nitrogen side. The computed VDE value for this structure, 5.18 eV, agrees well with the experiment. Unlike the n = 4 case, there are several possible hydrogen bonding networks that can be accommodated within the packing configuration associated with the ground state structure. Considering the overall trend across low-energy cluster structures for n = 5 cluster, as given by graph representations in Figure 5, we observe interesting similarity to corresponding structures in n = 4 case. Indeed the first two structures are generated by replacing bare SCN^- "nucleus" with the $SCN^-(H_2O)$ complex, and the last structure is obtained by replacing cyclic 4-water ring by its 5-ring counterpart.

$SCN^-(H_2O)_6$. In the n = 6 case, the transformation to the cubic structure is completed by insertion of the water molecule at the base of the pyramid on the sulfur side. Following the theme of previous cases (n = 4, 5), the structures of lowest energy clusters in the n = 6 case can also be represented as embedding lower order SCN^-–water clusters into cyclic water rings. The interesting feature of n = 6 cluster is the enhanced stability of the ground state cubic structure, with pronounced separation (+2.2 kcal/mol) from higher energy conformers.

$SCN^-(H_2O)_7$. The n = 7 SCN^-–water cluster maintains resemblance to cubic shape, but in this case the sulfur end becomes completely desolvated, and the nitrogen site of SCN^- occupies the corner of the cube made of water molecules. This class of structures allows for a number of possible hydrogen bonding configurations, which as shown in Figure 5 can lead to wide range variations in VDE values. The VDE value of 5.26 eV computed for the lowest energy structure (as shown in Figure 2) slightly underestimates the experimental estimate of 5.43 eV. The latter can be in principle matched to alternate hydrogen bonding arrangement with VDE value of 5.46 eV but higher total energy (+1.2 kcal/mol). As shown in Figure 5, the cubic-like arrangement persists in the next lowest energy class of structures, but in this case the sulfur also makes contact with one of the waters at the corner of cube. There are approximately 11 different structures within 1.2 kcal/mol range from the lowest energy structure (see the Supporting Information).

$SCN^-(H_2O)_8$. In the n = 8 cluster the lowest energy cluster takes the form of a pentagonal prism. The appearance of prism-like structures for an even number of waters seems to be a recurring theme for SCN^- water clusters. The computed VDE value of 5.53 eV is in reasonable agreement with the experimental value of 5.66 eV. While the ground state energy cluster can be represented as an embedding of $SCN^-(H_2O)_3$ cluster into pentamer ring water configuration, the higher energy clusters feature a 4-water ring surrounding $SCN^-(H_2O)_4$. There are approximately 19 different structures within 1.2 kcal/mol range from the lowest energy structure (see the Supporting Information).

Comparison of $SCN^-(H_2O)_n$ with Pure Water Clusters. One of the most interesting features about SCN^- solvated clusters becomes apparent when performing comparisons with pure water clusters. Indeed, one immediately observes that all lower energy solvated SCN^- structures can be generated from pure water clusters by the replacement of either the single water (utilizing the nitrogen site of SCN^-) or the water dimer (utilizing entire SCN^- molecule) (Figure 6). The latter

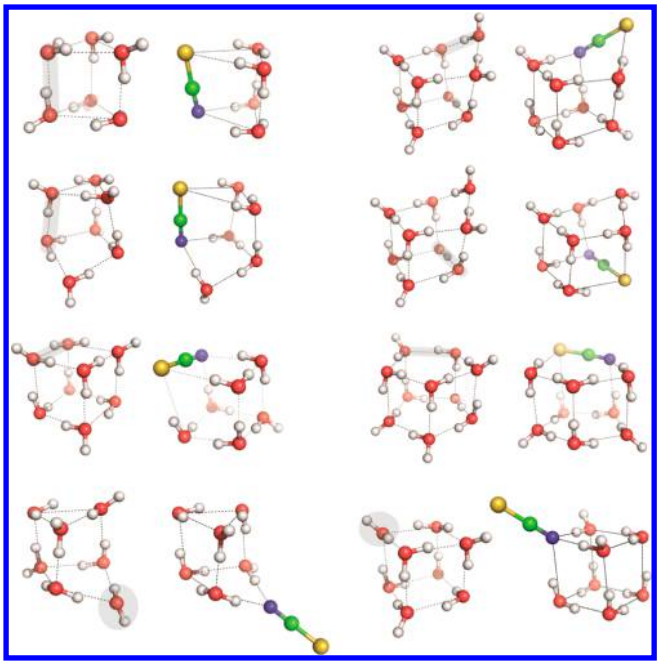

Figure 6. Comparison between selected ground state and low-lying isomers of SCN water clusters and pure water clusters. The highlighted region indicates the replacement position.

replacement is possible because of remarkable similarity between the SCN^- and the water dimer. Geometrically both have linear shapes with nearly the same total length: for SCN^- the S–N distance is 2.85 Å, and for water dimer the O–O distance is 2.88 Å. Analogous to water dimer, SCN^- can participate in hydrogen bonding at both ends of the molecule. Unlike the water molecule, which can serve either as hydrogen donor or acceptor, the only acceptor role is available for SCN^-. As a result, while the replacement preserves the packing of the original water clusters, it necessarily changes the local orientation of the hydrogen bonding network. The observed

DOI: 10.1021/acs.jpcb.5b07257
J. Phys. Chem. B XXXX, XXX, XXX–XXX

complementarity between solvated SCN^- clusters and native water structure suggests that the SCN^- solvation process is driven not just by the maximization of solute−water interactions but also by the stabilization of the internal water−water network. Typically the balance would be shifted toward solute−water interactions for kosmotropes, as charged solute would tend to reorganize water away from its native structure.[15,16,26,47,48] In the SCN^- case the perturbation of the water network appears to be limited to rewiring of hydrogen bonding on otherwise preserved spatial arrangement/packing of native water structure. Further insight into the interplay between solute−solvent and solvent−solvent stabilization effects can be gained from the analysis of cluster growth energy

$$\Delta E(n) = E(n) - E(n-1) - E_w$$

which is a difference between total energy of n and $n-1$ clusters referenced to the energy of the single water molecule (E_w). Of particular interest is the behavior of $\Delta E(n)$ for the neutral system ($\Delta E^{neutr}(n)$), where reduction in solute−water interactions allows us to expose the contribution from internal water network. As Figure 7 shows, $\Delta E^{neutr}(n)$ steadily gains in

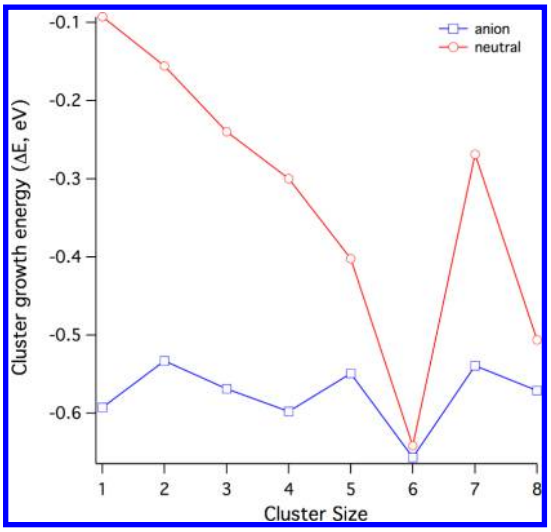

Figure 7. Calculated water binding energies (in eV) for anion and neutral SCN water clusters as a function of cluster size. The reference energy of water was set at −76.43413 au.

(negative) value reaching the peak at $n = 6$ cluster. This is in contrast to the behavior observed for the iodate solvation, where $\Delta E^{neutr}(n)$ shows an oscillatory behavior stemming from directional solute dipole water interactions.[15] This strongly suggests that the growth of solvated cluster in SCN case is accompanied by steady stabilization of the internal water network. The fact that this contribution peaks at the $n = 6$ case indicates that the cubic structure achieved in this case represents a particular stable water configuration. This is consistent with particularly large calculated band gap for $n = 6$ case and reduced experimental spectral width (see Figure 2). The enhanced stabilization of the water network in the $n = 6$ cluster also explains a peculiar flattening of experimental VDE value across $n = 5$ and $n = 6$ clusters. Indeed, this would imply that overall cluster stabilization for the $n = 6$ case is derived from the solvent part of the systems and not the solute−solvent stabilization effects that would be reflected in the increased value of VDE values.[16,48] It is also interesting to note that the stepwise cluster energy for SCN^-, $\Delta E^{anion}(n)$, remains largely constant from $n = 1$ to 8, because, as a chaotrope, SCN^- always resides either at the edge or corner of native water clusters (Figures 3−6). This behavior is distinctly different from the kosmotrope IO_3^-, where the absolute value of $\Delta E^{anion}(n)$ gradually reduced with number of waters as a result of charge screening effects due to stronger solute−solvent interactions in the smaller clusters and reorganizing ability of local water molecules by the solute.[15]

CONCLUSIONS

Size selective solvation of a negatively charged SCN^- molecule was investigated using combined photoelectron spectroscopy and theoretical modeling. Compared to previously investigated kosmotrope IO_3^-[15], the solvation of chaotropic SCN^- molecule exhibits a distinctly different cluster solvation pattern. Namely, the solvation process preserves the native packing arrangement, i.e., spatial three-dimensional arrangement of pure water clusters, but changes the local directionality of hydrogen bonds. Consistent with this, we observe monotonic increase of neutral cluster growth energy in the initial formation phase ($n = 1-6$) suggesting that the solvation of SCN^- is heavily driven by the stabilization of internal water network. The latter reaches its peak at the formation of highly stable cubic structure at $n = 6$, and identified experimentally through peculiar flattening of VDE and sizable reduction in spectral bandwidth.

In conclusion both experimental and computational results suggest that behavior of SCN^- indeed fits the definition of weakly hydrated ion, but its impact on local water structure is more subtle than would be implied by the "structure breaker" name. In fact, the insertion of SCN^- seems to preserve the spatial arrangement/packing of solvent molecules but changes the directionality of the hydrogen bonding network in the local vicinity of the solute. In that respect, the more appropriate description for SCN^- may be a "structure weakener", whereby the overall structure of the solvent remains intact but its stability is reduced due to inherent constraints on hydrogen bonding imposed by the presence of solute.

It should be pointed out that the cluster solvation of SCN^- presented here is still different from the bulk environment. Nevertheless, our results provide clear evidence that chaotropic properties of SCN^- are already apparent at the cluster level and bring further insight into the nature of this process.

ASSOCIATED CONTENT

Supporting Information

The Supporting Information is available free of charge on the ACS Publications website at DOI: 10.1021/acs.jpcb.5b07257.

Low lying isomers of $SCN^-(H_2O)_n$, $n = 7$ and 8 (PDF)

AUTHOR INFORMATION

Corresponding Authors

*E-mail: marat.valiev@pnnl.gov. Phone: 1-509-371-6459 .
*E-mail: xuebin.wang@pnnl.gov. Phone: 1-509-371-6132

Notes

The authors declare no competing financial interest.

ACKNOWLEDGMENTS

This work was supported by U.S. Department of Energy (DOE), Office of Science, Office of Basic Energy Sciences, Division of Chemical Sciences, Geosciences and Biosciences, and performed using EMSL, a national scientific user facility sponsored by DOE's Office of Biological and Environmental

DOI: 10.1021/acs.jpcb.5b07257
J. Phys. Chem. B XXXX, XXX, XXX−XXX

Research and located at Pacific Northwest National Laboratory, which is operated by Battelle Memorial Institute for the DOE.

REFERENCES

(1) Kunz, W.; Lo Nostro, P.; Ninham, B. W. The Present State of Affairs with Hofffieister Effects. *Curr. Opin. Colloid Interface Sci.* **2004**, *9*, 1−18.

(2) Zhang, Y. J.; Cremer, P. S. Interactions between Macromolecules and Ions: the Hofmeister Series. *Curr. Opin. Chem. Biol.* **2006**, *10*, 658−663.

(3) Tobias, D. J.; Hemminger, J. C. Chemistry - Getting Specific about Specific Ion Effects. *Science* **2008**, *319*, 1197−1198.

(4) Knipping, E. M.; Lakin, M. J.; Foster, K. L.; Jungwirth, P.; Tobias, D. J.; Gerber, R. B.; Dabdub, D.; Finlayson-Pitts, B. J. Experiments and Simulations of Ion-Enhanced Interfacial Chemistry on Aqueous NaCl Aerosols. *Science* **2000**, *288*, 301−306.

(5) Uejio, J. S.; Schwartz, C. P.; Duffin, A. M.; Drisdell, W. S.; Cohen, R. C.; Saykally, R. J. Characterization of Selective Binding of Alkali Cations with Carboxylate by X-ray Absorption Spectroscopy of Liquid Microjets. *Proc. Natl. Acad. Sci. U. S. A.* **2008**, *105*, 6809−6812.

(6) Jungwirth, P.; Tobias, D. J. Specific Ion Effects at the Air/Water Interface. *Chem. Rev.* **2006**, *106*, 1259−1281.

(7) Jungwirth, P.; Tobias, D. J. Ions at the Air/Water Interface. *J. Phys. Chem. B* **2002**, *106*, 6361−6373.

(8) Collins, K. D. Why Continuum Electrostatics Theories Cannot Explain Biological Structure, Polyelectrolytes or Ionic Strength Effects in Ion-Protein Interactions. *Biophys. Chem.* **2012**, *167*, 43−59.

(9) Baer, M. D.; Pham, V. T.; Fulton, J. L.; Schenter, G. K.; Balasubramanian, M.; Mundy, C. J. Is Iodate a Strongly Hydrated Cation? *J. Phys. Chem. Lett.* **2011**, *2*, 2650−2654.

(10) Baer, M. D.; Mundy, C. J. An Ab Initio Approach to Understanding the Specific Ion Effect. *Faraday Discuss.* **2013**, *160*, 89−101.

(11) Collins, K. D. Ions from the Hofmeister Series and Osmolytes: Effects on Proteins in Solution and in the Crystallization Process. *Methods* **2004**, *34*, 300−311.

(12) Omta, A. W.; Kropman, M. F.; Woutersen, S.; Bakker, H. J. Negligible Effect of Ions on the Hydrogen-Bond Structure in Liquid Water. *Science* **2003**, *301*, 347−349.

(13) Chen, X.; Yang, T.; Kataoka, S.; Cremer, P. S. Specific Ion Effects on Interfacial Water Structure near Macromolecules. *J. Am. Chem. Soc.* **2007**, *129*, 12272−12279.

(14) Vlachy, N.; Jagoda-Cwiklik, B.; Vacha, R.; Touraud, D.; Jungwirth, P.; Kunz, W. Hofmeister Series and Specific Interactions of Charged Headgroups with Aqueous Ions. *Adv. Colloid Interface Sci.* **2009**, *146*, 42−47.

(15) Wen, H.; Hou, G. L.; Kathmann, S. M.; Valiev, M.; Wang, X. B. Communication: Solute Anisotropy Effects in Hydrated Anion and Neutral Clusters. *J. Chem. Phys.* **2013**, *138*, 031101-1−4.

(16) Wang, X. B.; Yang, X.; Nicholas, J. B.; Wang, L. S. Bulk-like Features in the Photoemission Spectra of Hydrated Doubly Charged Anion Clusters. *Science* **2001**, *294*, 1322−1325.

(17) Wang, X. B.; Werhahn, J. C.; Wang, L. S.; Kowalski, K.; Laubereau, A.; Xantheas, S. S. Observation of a Remarkable Temperature Effect in the Hydrogen Bonding Structure and Dynamics of the $CN^-(H_2O)$ Cluster. *J. Phys. Chem. A* **2009**, *113*, 9579−9584.

(18) Markovich, G.; Pollack, S.; Giniger, R.; Cheshnovsky, O. Photoelectron Spectroscopy of Cl^-, Br^-, and I^- Solvated in Water Clusters. *J. Chem. Phys.* **1994**, *101*, 9344−9353.

(19) Dang, L. X.; Garrett, B. C. Photoelectron-Spectra of the Hydrated Iodine Anion from Molecular-Dynamics Simulations. *J. Chem. Phys.* **1993**, *99*, 2972−2977.

(20) Asmis, K. R.; Neumark, D. M. Vibrational Spectroscopy of Microhydrated Conjugate Base Anions. *Acc. Chem. Res.* **2012**, *45*, 43−52.

(21) Robertson, W. H.; Johnson, M. A. Molecular Aspects of Halide Ion Hydration: The Cluster Approach. *Annu. Rev. Phys. Chem.* **2003**, *54*, 173−213.

(22) Lisy, J. M. Spectroscopy and Structure of Solvated Alkali-Metal Ions. *Int. Rev. Phys. Chem.* **1997**, *16*, 267−289.

(23) Weber, J. M.; Kelley, J. A.; Nielsen, S. B.; Ayotte, P.; Johnson, M. A. Isolating the Spectroscopic Signature of a Hydration Shell with the Use of Clusters: Superoxide Tetrahydrate. *Science* **2000**, *287*, 2461−2463.

(24) Cabarcos, O. M.; Weinheimer, C. J.; Lisy, J. M.; Xantheas, S. S. Microscopic Hydration of the Fluoride Anion. *J. Chem. Phys.* **1999**, *110*, 5−8.

(25) Duncan, M. A. Frontiers in the Spectroscopy of Mass-Selected Molecular Ions. *Int. J. Mass Spectrom.* **2000**, *200*, 545−569.

(26) Bush, M. F.; Saykally, R. J.; Williams, E. R. Evidence for Water Rings in the Hexahydrated Sulfate Dianion from IR Spectroscopy. *J. Am. Chem. Soc.* **2007**, *129*, 2220−2221.

(27) Hurley, S. M.; Dermota, T. E.; Hydutsky, D. P.; Castleman, A. W. Dynamics of Hydrogen Bromide Dissolution in the Ground and Excited States. *Science* **2002**, *298*, 202−204.

(28) Li, X. A.; Wang, H. P.; Bowen, K. H. Photoelectron Spectroscopic Study of the Hydrated Nucleoside Anions: Uridine$^-(H_2O)_{(n=0-2)}$, Cytidine$^-(H_2O)_{(n=0-2)}$, and Thymidine$^-(H_2O)_{(n=0,1)}$. *J. Chem. Phys.* **2010**, *133*, 144304-1−5.

(29) Li, R. Z.; Liu, C. W.; Gao, Y. Q.; Jiang, H.; Xu, H. G.; Zheng, W. J. Microsolvation of LiI and CsI in Water: Anion Photoelectron Spectroscopy and Ab Initio Calculations. *J. Am. Chem. Soc.* **2013**, *135*, 5190−5199.

(30) Dribinski, V.; Barbera, J.; Martin, J. P.; Svendsen, A.; Thompson, M. A.; Parson, R.; Lineberger, W. C. Time-Resolved Study of Solvent-Induced Recombination in Photodissociated $IBr^-(CO_2)_n$ Clusters. *J. Chem. Phys.* **2006**, *125*, 133405-1−7.

(31) Yang, X.; Fu, Y. J.; Wang, X. B.; Slavicek, P.; Mucha, M.; Jungwirth, P.; Wang, L. S. Solvent-Mediated Folding of a Doubly Charged Anion. *J. Am. Chem. Soc.* **2004**, *126*, 876−883.

(32) Wang, X. B.; Yang, J.; Wang, L. S. Observation of Entropic Effect on Conformation Changes of Complex Systems under Well-Controlled Temperature Conditions. *J. Phys. Chem. A* **2008**, *112*, 172−175.

(33) Wang, X. B.; Wang, L. S. Development of a Low-Temperature Photoelectron Spectroscopy Instrument Using an Electrospray Ion Source and a Cryogenically Controlled Ion Trap. *Rev. Sci. Instrum.* **2008**, *79*, 073108-1−8.

(34) Valiev, M.; Bylaska, E. J.; Govind, N.; Kowalski, K.; Straatsma, T. P.; Van Dam, H. J. J.; Wang, D.; Nieplocha, J.; Apra, E.; Windus, T. L.; de Jong, W. NWChem: A Comprehensive and Scalable Open-Source Solution for Large Scale Molecular Simulations. *Comput. Phys. Commun.* **2010**, *181*, 1477−1489.

(35) Becke, A. D. A New Mixing of Hartree-Fock and Local Density-Functional Theories. *J. Chem. Phys.* **1993**, *98*, 1372−1377.

(36) Lee, C. T.; Yang, W. T.; Parr, R. G. Development of the Colle-Salvetti Correlation-Energy Formula into a Functional of the Electron-Density. *Phys. Rev. B: Condens. Matter Mater. Phys.* **1988**, *37*, 785−789.

(37) Dill, J. D.; Pople, J. A. Self-Consistent Molecular-Orbital Methods 0.15. Extended Gaussian-Type Basis Sets for Lithium, Beryllium, and Boron. *J. Chem. Phys.* **1975**, *62*, 2921−2923.

(38) Krishnan, R.; Binkley, J. S.; Seeger, R.; Pople, J. A. Self-Consistent Molecular-Orbital Methods 0.20. Basis Set for Correlated Wave-Functions. *J. Chem. Phys.* **1980**, *72*, 650−654.

(39) Alexandrova, A. N. H•$(H_2O)_n$ Clusters: Microsolvation of the Hydrogen Atom via Molecular Ab Initio Gradient Embedded Genetic Algorithm (GEGA). *J. Phys. Chem. A* **2010**, *114*, 12591−12599.

(40) Glendening, E. D.; Landis, C. R.; Weinhold, F. NBO 6.0: Natural Bond Orbital Analysis Program. *J. Comput. Chem.* **2013**, *34*, 1429−1437.

(41) Bradforth, S. E.; Kim, E. H.; Arnold, D. W.; Neumark, D. M. Photoelectron-Spectroscopy of C_n^-, NCO^-, and NCS^-. *J. Chem. Phys.* **1993**, *98*, 800−810.

(42) Deng, S. H. M.; Kong, X. Y.; Wang, X. B. Probing the Early Stages of Salt Nucleation-Experimental and Theoretical Investigations of Sodium/Potassium Thiocyanate Cluster Anions. *J. Chem. Phys.* **2015**, *142*, 024313-1−9.

DOI: 10.1021/acs.jpcb.5b07257
J. Phys. Chem. B XXXX, XXX, XXX−XXX

(43) Xantheas, S. S.; Burnham, C. J.; Harrison, R. J. Development of Transferable Interaction Models for Water. II. Accurate Energetics of the First Few Water Clusters from First Principles. *J. Chem. Phys.* **2002**, *116*, 1493−1499.
(44) Miliordos, E.; Xantheas, S. S. An Accurate and Efficient Computational Protocol for Obtaining the Complete Basis Set Limits of the Binding Energies of Water Clusters at the MP2 and CCSD(T) Levels of Theory: Application to $(H_2O)_m$, m = 2−6, 8, 11, 16, and 17. *J. Chem. Phys.* **2015**, *142*, 234303-1−15.
(45) Robertson, W. H.; Diken, E. G.; Price, E. A.; Shin, J. W.; Johnson, M. A. Spectroscopic Determination of the OH^- Solvation Shell in the $OH^-\bullet(H_2O)_n$ Clusters. *Science* **2003**, *299*, 1367−1372.
(46) Fournier, J. A.; Johnson, C. J.; Wolke, C. T.; Weddle, G. H.; Wolk, A. B.; Johnson, M. A. Vibrational Spectral Signature of the Proton Defect in the Three-Dimensional $H^+(H_2O)_{21}$ Cluster. *Science* **2014**, *344*, 1009−1012.
(47) Zhou, J.; Santambrogio, G.; Brummer, M.; Moore, D. T.; Meijer, G.; Neumark, D. M.; Asmis, K. R. Infrared Spectroscopy of Hydrated Sulfate Dianions. *J. Chem. Phys.* **2006**, *125*, 111102-1−4.
(48) Wang, X. B.; Sergeeva, A. P.; Yang, J.; Xing, X. P.; Boldyrev, A. I.; Wang, L. S. Photoelectron Spectroscopy of Cold Hydrated Sulfate Clusters, $SO_4^{2-}(H_2O)_n$ (n = 4−7): Temperature-Dependent Isomer Populations. *J. Phys. Chem. A* **2009**, *113*, 5567−5576.

DOI: 10.1021/acs.jpcb.5b07257
J. Phys. Chem. B XXXX, XXX, XXX−XXX